Progress In Electromagnetics Research, PIER 69, 127–144, 2007

NEURAL MODELS FOR COPLANAR STRIP LINE SYNTHESIS

C. Yildiz, K. Guney, M. Turkmen, and S. Kaya

Department of Electrical and Electronics Engineering
Faculty of Engineering
Erciyes University
38039, Kayseri, Turkey

Abstract—Simple and accurate models based on artificial neural networks (ANNs) are presented to accurately determine the physical dimensions of coplanar strip lines (CPSs). Five learning algorithms, Levenberg-Marquardt (LM), bayesian regularization (BR), quasi-Newton (QN), conjugate gradient with Fletcher (CGF), and scaled conjugate gradient (SCG), are used to train the neural models. The neural results are compared with the results of the quasi-static analysis and the synthesis formulas available in the literature. The accuracy of the neural model trained by LM algorithm is found to be better than 0.24% for 10614 CPS samples.

1. INTRODUCTION

CPSs, like coplanar waveguides, allow easy connections for series and shunt solid state devices. Good propagation, small dispersion, comparably intensive to substrate thickness, and simple implementation of open or short-ended strips are the basic characteristics of CPSs. Briefly, CPSs support all of the advantages of the conventional coplanar waveguides. Furthermore, the structure of CPSs is very useful for radio frequency and microwave integrated circuits (MICs), especially balanced circuits due to its inherent balanced nature [1]. Various symmetric and asymmetric CPSs on single or multilayer substrates were analyzed to obtain closed-form expressions for quasi-TEM parameters using quasi-static methods [2–6] and to determine dispersion characteristics of CPSs with the use of full-wave methods [7–9]. While full-wave methods are the most accurate tools for obtaining the transmission-line characteristics and are also analytically extensive, the quasi-static methods are quite simple and lead to closed-form expressions suitable for computer-aided design (CAD) software packages, but the latter methods do not consider the dispersive nature of generic transmission lines. Consequently, the approximation of quasi-static methods becomes worse as the transmission line becomes dispersive. However, it was shown by Knorr and Kuchler [7] that the CPS parameters are only slightly sensitive to variations of the frequency for CPSs with dimensions not exceeding the substrate thickness for nearly the whole microwave region. For this reason, the quasi-static methods provide simulation accuracy that is comparable with the full-wave methods for frequencies up to 20 GHz and even up to 40 GHz.

Most of the conventional models for various CPSs are the analysis models [2–9] that have been used to determine the characteristic parameters of CPS structures. The synthesis models were also presented in the literature [10–12]. These synthesis models are directly used to obtain the physical dimensions of CPS structures for the required design specifications. The model proposed by Deng et al. [10] is mathematically complex. The models presented by Yildiz [11] and Yildiz et al. [12] are simple but do not have very good accuracy. Hence, they are not very attractive for the CPS synthesis.

This paper presents simple and accurate synthesis models based on ANNs in order to very accurately compute the physical dimensions of CPS structures for the required design specifications. ANN is a very powerful approach for building complex and nonlinear relationship between a set of input and output data [13]. Analysis [14–20] and synthesis models [21–24] based on ANNs have been presented for various coplanar transmission lines. In these applications, ANNs have more general functional forms and are usually better than the classical techniques; also, they provide simplicity in real-time operation. One of the most powerful uses of ANNs is function approximation (curve-fitting). A main characteristic of this solution is that a function (f) to be approximated is given not explicitly, but implicitly through a set of input-output pairs called training data sets.

Neural model for the CPS synthesis was introduced for the first time by Salivahanan et al. [24]. This neural model has some disadvantages. First of all, it can be used in the narrow range: $2 \leq \varepsilon_r \leq 13$, $0.5 \leq S/H \leq 5$, and $0.5 \leq W/H \leq 5$. It is not possible to design CPSs having small characteristic impedances ($Z_0 < 70\,\Omega$) for the ranges of $\varepsilon_r < 13$, $0.5 < S/H$, and $0.5 < W/H$. Thus, this neural model is not suitable for practical ranges. Moreover, the neural model proposed in [24] was trained using only one learning algorithm.

In this paper, simple and accurate neural models with a very wide range of usage for CPS synthesis are presented within the following design-parameter ranges: $2.2 \leq \varepsilon_r \leq 50$, $0.01 \leq S/H \leq 1.86$, and

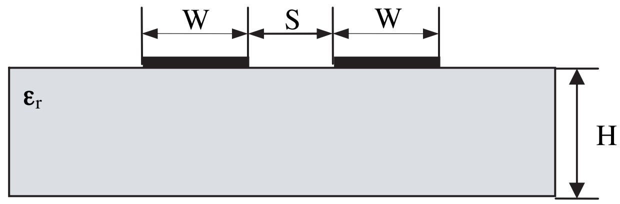

Figure 1. Configuration of a CPS.

$0.01 \leq W/H \leq 5.59$. These neural models were trained with LM [25], BR [26], QN [27], CGF [28], and SCG [29] learning algorithms to obtain better performance and faster convergence with a simpler structure. For the validation of the neural models proposed in this paper, the neural synthesis results have been compared with the results of the quasi-static analysis [6] and the synthesis formulas proposed by other researchers [10–12].

2. SYNTHESIS FORMULAS FOR CPSs

A CPS with a finite dielectric thickness configuration is depicted in Fig. 1, where S, W, H, and ε_r represent the slot width, strip width, substrate thickness, and relative dielectric constant of the substrate material, respectively. All the conductors are assumed to be infinitely thin and perfectly conducting. The following synthesis formula proposed in [10] calculates the strip width W for a given substrate (H, ε_r) and required characteristic impedance Z_0 by choosing an appropriate slot width S.

$$W = \frac{S}{G(\varepsilon_r, H, Z_0, S)} \tag{1}$$

with

$$G = \begin{cases} \left[\frac{1}{8} \cdot \exp\left(\frac{60 \cdot \pi^2}{Z_0 \cdot \sqrt{\varepsilon_{re}}}\right) - \frac{1}{2}\right]^{-1} & \text{for } Z_0 \leq \frac{\eta_0}{\sqrt{2(\varepsilon_r+1)}} \\ \frac{1}{4} \cdot \exp\left(\frac{Z_0 \cdot \sqrt{\varepsilon_{re}}}{120}\right) + \exp\left(-\frac{Z_0 \cdot \sqrt{\varepsilon_{re}}}{120}\right) - 1 & \text{for } Z_0 > \frac{\eta_0}{\sqrt{2(\varepsilon_r+1)}} \end{cases} \tag{2a}$$

where η_0 is the intrinsic impedance of free space and ε_{re} is the relative effective dielectric constant given by

$$\varepsilon_{re} = \varepsilon_{re}(\varepsilon_r, H, Z_0, S) = T_1 \left(1 + \frac{\varepsilon_r - 1}{Z_0 \cdot \sqrt{\varepsilon_r + 1}} T_2\right) \tag{2b}$$

with

$$\begin{aligned} T_1 &= \sec h\left\{\frac{\pi\cdot\varepsilon_r^5}{(\varepsilon_r+1)^6}\cdot\left(\frac{60}{Z_0}\right)^2\right.\\ &\quad\left.\cdot\exp\left[\left(1+\varepsilon_r\cdot\left(\frac{Z_0}{121}\right)^4\cdot\frac{S}{Q\cdot H}\right)\ln\left(\frac{S}{Q\cdot H}\right)\right]\right\} \end{aligned} \tag{2c}$$

$$T_2 = \begin{cases} 84.85\cdot\ln\left(2\cdot\frac{1+g}{1-g}\right) & \text{for } 0.841\leq g\leq 1\\ 837.5\cdot\left[\ln\left(2\cdot\frac{1+\sqrt[4]{1-g^4}}{1-\sqrt[4]{1-g^4}}\right)\right]^{-1} & \text{for } 0<g\leq 0.841 \end{cases} \tag{2d}$$

$$g = \left\{\frac{\exp\left(\dfrac{\pi\cdot(1+1/Q)\cdot S}{2\cdot H}\right)-\exp\left(\dfrac{\pi\cdot S}{2\cdot Q\cdot H}\right)}{\exp\left(\dfrac{\pi\cdot(1+2/Q)\cdot S}{2\cdot H}\right)-1}\right\}^{1/2} \tag{2e}$$

and

$$Q = G\Big|_{\varepsilon_{re}=\frac{\varepsilon_r+1}{2}} \tag{2f}$$

The value of G in eq. (1) can also be obtained from the following eqs. (3) and (4) proposed in [11] and [12], respectively.

$$G=\begin{cases} 20.385\cdot\exp\left\{-1.241\cdot\left(\frac{\eta_0}{Z_0\sqrt{\varepsilon_r+1}}\right)\right.\\ \quad\left.\cdot\left(1+\exp\left(0.275\cdot\left(\frac{S}{H}\right)^{0.65}\cdot\left(\frac{\varepsilon_r-0.88}{\varepsilon_r}\right)\right)^{0.53}\right)\right\}\\ \qquad\qquad\qquad\qquad\text{for } Z_0<\frac{\eta_0}{\sqrt{2(\varepsilon_r+1)}}\\ 24.218\cdot\left\{\left(\frac{\eta_0}{Z_0\sqrt{\varepsilon_r+1}}\right)\left[1+\exp\left(0.22\cdot\left(\frac{S}{H}\right)^{1.30}\cdot\left(\frac{\varepsilon_r-1}{\varepsilon_r}\right)\right)\right]\right\}^{-4.07}\\ \qquad\qquad\qquad\qquad\text{for } Z_0\geq\frac{\eta_0}{\sqrt{2(\varepsilon_r+1)}} \end{cases} \tag{3}$$

and

$$G=\begin{cases} -1.0083\cdot\exp\left(\left(\frac{S}{H}\right)^{0.4261}\cdot\varepsilon_r^{2.3613}\left(\frac{Z_0}{\eta_0}\right)^{1.1966}\right) \\ +\exp\left(9.7854\cdot\left(\frac{Z_0}{\eta_0}\right)^{4.0479}\right)+3.7066\cdot\varepsilon_r^{2.0667}\left(\frac{Z_0}{\eta_0}\right)^{4.2467} \\ \qquad\qquad\qquad\text{for } Z_0<\frac{\eta_0}{\sqrt{2(\varepsilon_r+1)}} \\ -0.4394\cdot\exp\left(\left(\frac{S}{H}\right)^{0.1753}\cdot\varepsilon_r^{-0.0848}\left(\frac{Z_0}{\eta_0}\right)^{-0.0524}\right) \\ +\exp\left(1.8679\cdot\left(\frac{Z_0}{\eta_0}\right)^{1.8822}\right)+1.2015\cdot\varepsilon_r^{2.1294}\left(\frac{Z_0}{\eta_0}\right)^{4.2530} \\ \qquad\qquad\qquad\text{for } Z_0\geq\frac{\eta_0}{\sqrt{2(\varepsilon_r+1)}} \end{cases} \tag{4}$$

The following synthesis formula presented by Deng et al. [10] calculates the slot width S for a given substrate (H, ε_r) and required characteristic impedance Z_0 by choosing an appropriate strip width W.

$$S = W\cdot G(\varepsilon_r, H, Z_0, W) \tag{5}$$

with

$$G=\begin{cases} \left[\frac{1}{8}\cdot\exp\left(\frac{60\cdot\pi^2}{Z_0\cdot\sqrt{\varepsilon_{ref}}}\right)-\frac{1}{2}\right]^{-1} & \text{for } Z_0\leq\frac{\eta_0}{\sqrt{2(\varepsilon_r+1)}} \\ \frac{1}{4}\cdot\exp\left(\frac{Z_0\cdot\sqrt{\varepsilon_{ref}}}{120}\right)+\exp\left(-\frac{Z_0\cdot\sqrt{\varepsilon_{ref}}}{120}\right)-1 & \text{for } Z_0>\frac{\eta_0}{\sqrt{2(\varepsilon_r+1)}} \end{cases} \tag{6a}$$

where

$$\varepsilon_{ref}=\varepsilon_{ref}(\varepsilon_r, H, Z_0, W)=T_3\left(1+\frac{\varepsilon_r-1}{Z_0\cdot\sqrt{\varepsilon_r+1}}T_4\right) \tag{6b}$$

with

$$T_3 = 1+\tanh\left\{\frac{Z_0^2\cdot\varepsilon_r^7}{720\cdot\pi^3\cdot(\varepsilon_r+1)^8}\cdot\exp\left[\left(1+0.0004\cdot\varepsilon_r\cdot Z_0\cdot\frac{W}{H}\right)\ln\left(\frac{W}{H}\right)\right]\right\} \tag{6c}$$

$$T_4 = \begin{cases} 84.85 \cdot \ln\left(2 \cdot \frac{1+t}{1-t}\right) & \text{for } 0.841 \leq t \leq 1 \\ 837.5 \cdot \left[\ln\left(2 \cdot \frac{1+\sqrt[4]{1-t^4}}{1-\sqrt[4]{1-t^4}}\right)\right]^{-1} & \text{for } 0 < t \leq 0.841 \end{cases} \tag{6d}$$

$$t = \left\{ \frac{\exp\left(\dfrac{\pi \cdot (1+P) \cdot W}{2 \cdot H}\right) - \exp\left(\dfrac{\pi \cdot W}{2 \cdot H}\right)}{\exp\left(\dfrac{\pi \cdot (2+P) \cdot W}{2 \cdot H}\right) - 1} \right\}^{1/2} \tag{6e}$$

and

$$P = G\Big|_{\varepsilon_{ref} = \frac{\varepsilon_r + 1}{2}} \tag{6f}$$

The value of G in eq. (5) can also be determined from the following eqs. (7) and (8) proposed in [11] and [12], respectively.

$$G = \begin{cases} 7.234 \cdot \exp\left\{-1.054 \cdot \left(\frac{\eta_0}{Z_0\sqrt{\varepsilon_r+1}}\right)\left[1+\exp\left(\frac{0.072 \cdot W \cdot (\varepsilon_r - 1.22}{H \cdot \varepsilon_r}\right)^{0.75}\right]\right\} \\ \qquad \text{for } Z_0 < \frac{\eta_0}{\sqrt{2(\varepsilon_r+1)}} \\ 21.385 \cdot \left\{\left(\frac{\eta_0}{Z_0\sqrt{\varepsilon_r+0.86}}\right) \cdot \left[1+\exp\left(\frac{0.1 \cdot W \cdot (\varepsilon_r - 1.52)}{H \cdot \varepsilon_r}\right)^{0.68}\right]\right\}^{-3.753} \\ \qquad \text{for } Z_0 \geq \frac{\eta_0}{\sqrt{2(\varepsilon_r+1)}} \end{cases} \tag{7}$$

and

$$G = \begin{cases} -1.0050 \cdot \exp\left(\left(\frac{W}{H}\right)^{0.6229} \cdot \varepsilon_r^{4.7557}\left(\frac{Z_0}{\eta_0}\right)^{2.3716}\right) \\ \quad + \exp\left(8.4331 \cdot \left(\frac{Z_0}{\eta_0}\right)^{4.2339}\right) + 3.5531 \cdot \varepsilon_r^{2.1547}\left(\frac{Z_0}{\eta_0}\right)^{4.4647} \\ \qquad \text{for } Z_0 < \frac{\eta_0}{\sqrt{2(\varepsilon_r+1)}} \\ -0.9255 \cdot \exp\left(\left(\frac{W}{H}\right)^{0.4156} \cdot \varepsilon_r^{3.1556}\left(\frac{Z_0}{\eta_0}\right)^{1.3762}\right) \\ \quad + \exp\left(1.6588 \cdot \left(\frac{Z_0}{\eta_0}\right)^{2.0995}\right) + 2.2560 \cdot \varepsilon_r^{1.8277}\left(\frac{Z_0}{\eta_0}\right)^{3.8805} \\ \qquad \text{for } Z_0 \geq \frac{\eta_0}{\sqrt{2(\varepsilon_r+1)}} \end{cases} \tag{8}$$

The synthesis formulas given above are valid for the ranges of $S/H \leq 10/[3(1+\ln\varepsilon_r)]$, $W/H \leq 10/(1+\ln\varepsilon_r)$, and $2.2 \leq \varepsilon_r \leq 50$.

3. ARTIFICIAL NEURAL NETWORKS (ANNs)

ANN represents a promising modeling technique, especially for data sets having non-linear relationships that are frequently encountered in engineering [13, 30–35]. In the course of developing an ANN model, the architecture of ANN and the learning algorithm are the two most important factors. ANNs have many structures and architectures [13]. The class of ANN and/or architecture selected for a particular model implementation depends on the problem to be solved. After several experiments using different architectures coupled with different training algorithms, in this paper, the multilayered perceptron (MLP) neural network architecture [13] is used in calculating the physical dimensions of CPSs. MLPs have a simple layer structure in which successive layers of neurons are fully interconnected, with connection weights controlling the strength of the connections. The MLP comprises an input layer, an output layer, and a number of hidden layers. MLPs can be trained using many different learning algorithms [13]. In this article, the five learning algorithms described briefly in the following sections were used to train the MLPs.

3.1. Levenberg-Marquardt (LM) Algorithm

This algorithm is a least-squares estimation algorithm based on the maximum neighborhood idea [25]. The error function $E(w)$ is given by

$$E(w) = \sum_{i=1}^{m} e_i^2(w) = \|g(w)\|^2 \tag{9}$$

with

$$e_i^2(w) = (y_{di} - y_i)^2 \tag{10}$$

where $g(w)$ is a function containing the individual error terms, y_{di} is the desired value of output neuron i, and y_i is the actual output of that neuron.

It is assumed that function $g(w)$ and its Jacobian J are known at point w. The LM algorithm is used to calculate the weight vector w such that $E(w)$ is minimum. A new weight vector w_{k+1} can be determined from the previous weight vector w_k as follows:

$$w_{k+1} = w_k + \delta w_k \tag{11}$$

with

$$\delta w_k = -\left(J_k^T g(w_k)\right)\left(J_k^T J_k + \lambda I\right)^{-1} \tag{12}$$

where k is the number of the iterations, J_k is the Jacobian of $g(w_k)$ evaluated by taking derivative of $g(w_k)$ with respect to w_k, λ is the Marquardt parameter, and I is the identity matrix.

3.2. Bayesian Regularization (BR) Algorithm

This algorithm updates the weight and bias values according to the LM optimization and minimizes a linear combination of squared errors and weights [26]. It also modifies the linear combination so that at the end of training the resulting network has good generalization qualities. Backpropagation is used to compute the Jacobian JX of performance with respect to the weight and bias variables X. Each variable is adjusted according to LM:

$$dX = -[(JX)(JX) + \lambda I]^{-1}[(JX)E] \tag{13}$$

3.3. Quasi-Newton (QN) Algorithm

This algorithm consists of the following steps [27]:

1. Set a search direction $s_k = -B_k \cdot g_k$,
2. $w_{k+1} = w_k + \eta \cdot s_k$,
3. Update B_k giving B_{k+1}

where B is the approximate inverse second derivative matrix, g is the first derivative term, η is a scalar step length parameter, and s is an updating direction. The major concept of the algorithm is the updating strategy for the approximate inverse second derivative matrix. B_{k+1} is obtained by using the following formula:

$$B_{k+1} = B + \left(1 + \frac{\gamma^T B\gamma}{\sigma^T\gamma}\right)\frac{\sigma\sigma^T}{\sigma^T\gamma} - \frac{\sigma\gamma^T B + B\gamma\sigma^T}{\sigma^T\gamma} \tag{14}$$

with

$$\gamma_k = g_{k+1} - g_k \tag{15}$$

and

$$\sigma_k = \eta s_k = w_{k+1} - w_k \tag{16}$$

The initial matrix B is usually selected to be a unit matrix.

3.4. Conjugate Gradient of Fletcher-Reeves (CGF) Algorithm

This algorithm updates weight and bias values according to the formulas proposed by Fletcher and Reeves [28]. The method of conjugate directions can be used to minimize a positive definite quadratic function in n steps. The minimum of E is determined by a sequence of linear searches along directions $s_k,\ k = 1, 2, , \dots , n$

$$w_{k+1} = w_k = \mu_k s_k \tag{17}$$

with

$$\mu_k = \arg\ \min_\mu E(w_k + \mu s_k) \tag{18}$$

and

$$s_{k+1} = -d(w_{k+1}) + \beta_k s_k \tag{19}$$

where $d(w_k) = \frac{\partial E(w)}{\partial w_{ij}}\Big|_{w=w_k}$, and β_k is given by [28]:

$$\beta_k = \frac{d(w_{k+1})^T d(w_{k+1})}{d(w_k)^T d(w_k)} \tag{20}$$

3.5. Scaled Conjugate Gradient (SCG) Algorithm

This algorithm [29] is an implementation of avoiding the complicated line search procedure of conventional conjugate gradient algorithm. For the SCG algorithm, the Hessian matrix is approximated by using the following formula

$$E''(w_k)s_k \approx \frac{E'(w_k + \sigma_k s_k) - E'(w_k)}{\sigma_k} + \lambda_k s_k \tag{21}$$

where E' and E'' are the first and second derivative information of error function $E(w_k)$. The other terms s_k, σ_k and λ_k represent the search direction, the parameter controlling the change in weight for second derivative approximation, and the parameter for regulating the indefiniteness of the Hessian, respectively.

4. SYNTHESIS MODELS BASED ON ANNs FOR CPSs

In this paper, two simple and accurate neural models are proposed for CPS synthesis. The first neural model computes the strip width W

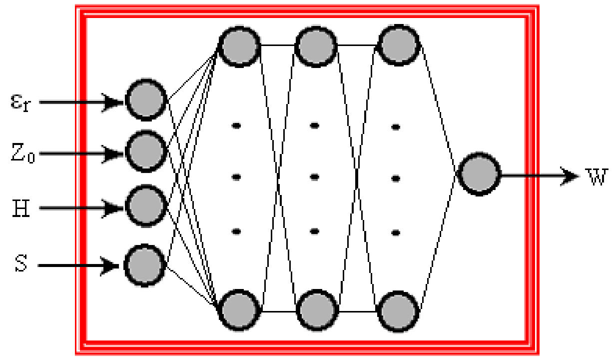

(a)

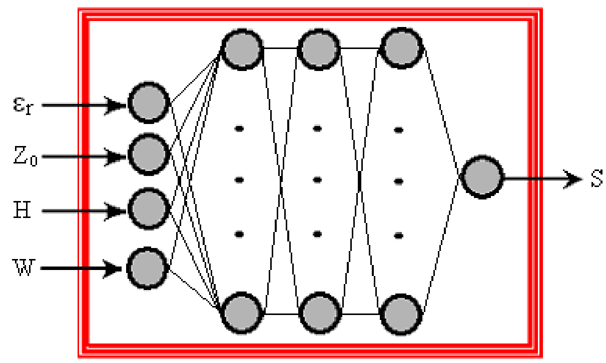

(b)

Figure 2. Neural models for CPS synthesis: (a) the first neural model used to calculate the strip width of a CPS; (b) the second neural model used to calculate the slot width of a CPS.

for a given substrate (H, ε_r) and required characteristic impedance Z_0 by choosing an appropriate slot width S. The second neural model calculates the slot width S for a given substrate (H, ε_r) and required characteristic impedance Z_0 by choosing an appropriate strip width W. Fig. 2(a) and 2(b) show the first and second neural models used for neural computation of the strip width and slot width of CPSs, respectively.

ANN models are a kind of black box models, whose accuracy depends on the data presented to it during training. A good collection of the training data, i.e., data which is well-distributed, sufficient, and accurately simulated, is the basic requirement to obtain an accurate model. For microwave applications, there are two types of data generators, namely measurement and simulation. The selection of a data generator depends on the application and the availability of the data generator. The training data sets used in this paper were obtained from the respective quasi-static analysis [6] and contain 7839 samples. The design parameter ranges of the CPSs in these samples are $2.2 \leq \varepsilon_r \leq 50$, $0.01 \leq S/H \leq 1.86$, $0.01 \leq W/H \leq 5.59, 200\,\mu\text{m} \leq H \leq 1250\,\mu\text{m}$, and respective characteristic impedance $30\Omega \leq Z_0 \leq 600\Omega$. 2775 data sets, which are completely different from training data sets, were used to test the ANNs. The train and test data sets were generated under the following constraints: normalized strip width $W/H \leq 10/(1 + \ln \varepsilon_r)$, normalized slot width $S/H \leq 10/[3(1 + \ln \varepsilon_r)]$, and relative dielectric constant $2.2 \leq \varepsilon_r \leq 50$. The values of the input and the output data sets were scaled between 0 and 1 before training.

The aim of the training process is to minimize the training error between the target output and the actual output of the ANN. Training the ANNs with the use of a learning algorithm to calculate strip widths W or the slot widths S of CPSs involves presenting them sequentially and/or randomly with different sets (ε_r, Z_0, H, and S or W) and corresponding parameters (W or S). First, the input vectors (ε_r, Z_0, H, and S or W) are presented to the input neurons and output vector (W or S) is computed. ANN output is then compared to the known output of the training data sets and errors are computed. Error derivatives are then calculated and summed up for each weight until all the training examples have been presented to the network. These error derivatives are then used to update the weights for neurons in the model. Training proceeds until errors are lower than prescribed values.

Selection of training parameters and the entire training process mostly depend on experience besides the type of problem at hand. After several trials, it was found in this paper that three hidden layered network was achieved the task in high accuracy. The most suitable network configuration found was $4 \times 4 \times 12 \times 12 \times 1$. It means that the numbers of neurons were 4, 4, 12, 12, and 1 for the input layer, the first, second, and third hidden layers and the output layer, respectively. The tangent hyperbolic and logarithmic sigmoid activation functions were used in the first hidden layer, and the second and third hidden layers, respectively. The linear activation function was used in the input and output layers. Initial weights of the neural models were set up randomly.

5. NUMERICAL RESULTS AND DISCUSSION

ANNs have been successfully used to compute the strip width or slot width of a CPS for a given substrate material and required characteristic impedance by choosing an appropriate slot or strip width. In order to obtain better performance, faster convergence, and a simpler structure, ANN models were trained with the LM, BR, QN, CGF and SCG learning algorithms. The training and test root mean square (RMS) errors obtained from the first and second neural models are given in Table 1 for the strip widths and slot widths of CPSs, respectively. It is clear from Table 1 that the results of the neural models trained by the LM and BR algorithms are better than those of the neural models trained by QN, CGF, and SCG algorithms. Among the neural models, the worst result was obtained from the neural model trained using the SCG algorithm. The RMS error values clearly show that the neural models can be used in calculating the physical dimensions of CPSs.

Table 1. Training and test RMS errors of neural models.

Learning algorithms	First neural model		Second neural model	
	RMS errors in training for W (μm)	RMS errors in testing for W (μm)	RMS errors in training for S (μm)	RMS errors in testing for S (μm)
LM	0.004360	0.007693	0.000441	0.007861
BR	0.000832	0.001815	0.004085	0.022049
QN	0.060029	0.106599	0.105271	0.685054
CGF	0.404361	0.037889	0.962608	0.265909
SCG	1.360000	0.278000	1.723964	1.080720

In order to validate the neural models for CPS synthesis, comprehensive comparisons have been made. In these comparisons, the results obtained from the first and second neural models trained by LM algorithm are compared with three other approaches from the literature. These are the results of the respective quasi-static analysis [6], and two CAD models [10, 12] which are known as the best accurate tools for CPS synthesis.

Comparisons among the results of first neural model, the synthesis formula proposed by Deng et al. [10], the synthesis formula proposed by Yildiz et al. [12], and the quasi-static analysis [6] are presented graphically in Fig. 3. This figure shows the contours of normalized slot width S/H versus normalized strip width W/H for various characteristic impedance values for a given substrate material ($\varepsilon_r = 12.9$ and $H = 200\,\mu$m). Similar comparisons are made for the second neural model; the results of the synthesis formulas [10, 12] and quasi-static analysis [6], and obtained contours are shown in Fig. 4 for various characteristic impedance values for a given substrate material ($\varepsilon_r = 12.9$ and $H = 200\,\mu$m). In these figures, the validations of

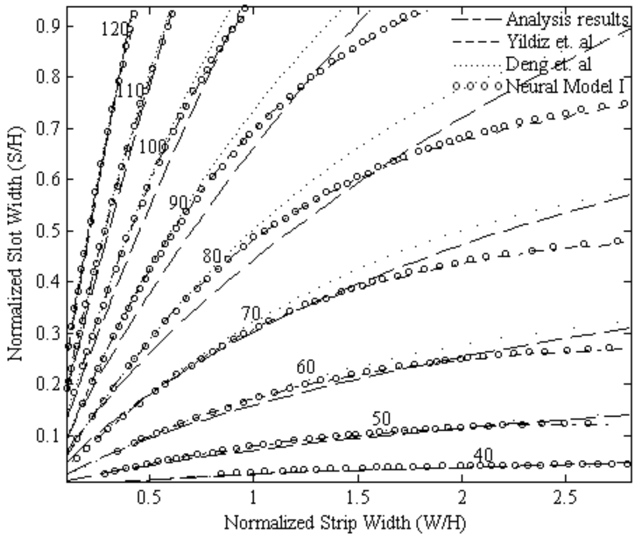

Figure 3. Comparisons among the neural synthesis results $W(Z_0, S)$ using the first neural model, the synthesis results $W(Z_0, S)$ of Deng et al. [10] and Yildiz et al. [12], and the quasi-static analysis [6] contours of $Z_0(S, W)$, with $\varepsilon_r = 12.9$ and $H = 200\,\mu$m.

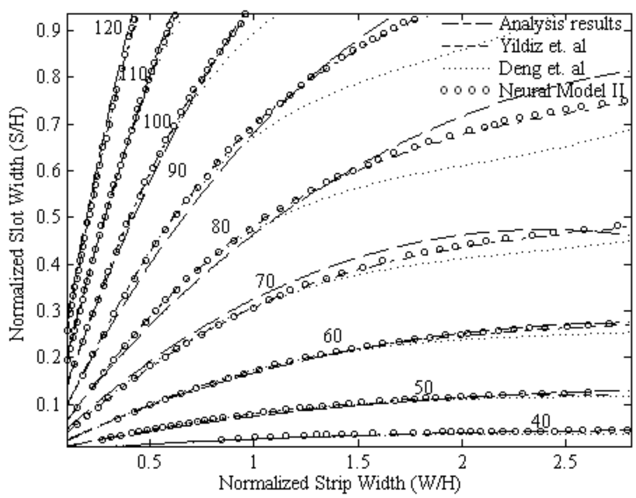

Figure 4. Comparisons among the neural synthesis results $S(Z_0, W)$ using the second neural model, the synthesis results $S(Z_0, W)$ of Deng et al. [10] and Yildiz et al. [12], and the quasi-static analysis [6] contours of $Z_0(S, W)$, with $\varepsilon_r = 12.9$ and $H = 200\,\mu$m.

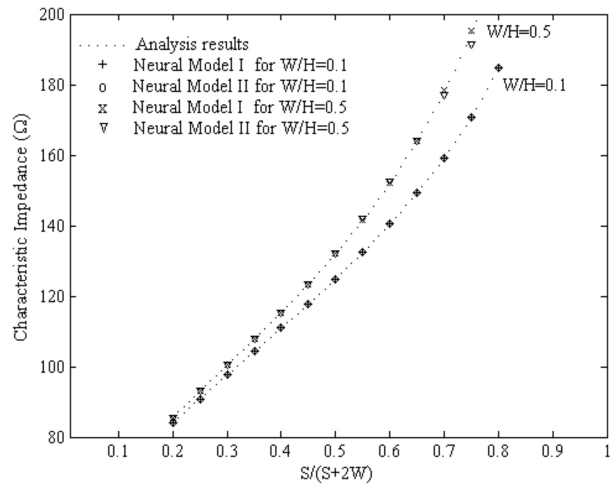

Figure 5. Comparisons among the characteristic impedances calculated by using the first synthesis neural model $Z_0(W, \varepsilon_r, H)$ for a given S; the second synthesis neural model $Z_0(S, \varepsilon_r, H)$ for a given W; and the quasi-static analysis [6] $Z_0(W, S)$, with $\varepsilon_r = 10.2$.

the presented neural models are considered for all possible values of normalized strip width W/H and normalized slot width S/H within the ranges of $W/H \leq 10/(1 + \ln \varepsilon_r)$ for the first neural model, and $S/H \leq 10/[3(1 + \ln \varepsilon_r)]$for the second neural model. It is apparent from Figs. 3 and 4 that the results of the neural models are in excellent agreement with those of the quasi-static analysis, whereas there is no good agreement between the results of quasi-static analysis and the synthesis CAD models [10, 12], especially in the extreme ranges of the normalized strip width W/H and normalized slot width S/H. A similar perfect agreement between the results of the neural models and quasi-static analysis is also achieved for all CPS structures to be designed with different electrical parameters and physical dimensions. It was found that the average percentage error values of the neural models, the synthesis formulas proposed by Deng et al. [10], by Yildiz [11], and by Yildiz et al. [12] are 0.24%, 0.84%, 1.43%, and 1.25% for all possible 10614 CPS structures, respectively. These results certainly show that the proposed neural models for CPS synthesis are more accurate than the synthesis formulas available in the literature.

In order to illustrate the self-consistent agreement between the first and second neural models and the validation of the neural models, another comparison is made for the characteristic impedances of CPSs having different substrate materials and different normalized strip width W/H values. In this comparison, the results obtained from the first and second neural models are compared with the results of quasi-static analysis. The results obtained from the first and second neural models, and the quasi-static analysis are given in Fig. 5 for the characteristic impedance of a CPS having two different W/H values with respect to the shape ratio $S/(S+2W)$. It is seen from Fig. 5 that the results of the proposed first and second neural models are very close to each other, and there is an excellent agreement between the results of neural models and the results of the quasi-static analysis.

Finally, the self-consistent agreement between the first and second neural models has been clearly seen throughout the comparisons. Although the neural models proposed in this work are trained with the data sets obtained from respective quasi-static analysis, an earlier investigation [7] showed that they can be used for the design of GaAs monolithic MICs up to a frequency range of 20 GHz and even 40 GHz. This is why the proposed neural models for CPS synthesis are valid for this frequency range.

6. CONCLUSION

Accurate and simple neural models are presented to compute the physical dimensions of CPSs for the required design specifications. These models have been developed by training the neural network with the numerical results of quasi-static analysis in the required ranges of model input variables. Neural models were trained by using five different learning algorithms to obtain better performance and faster convergence with a simpler structure. It was shown that the results of the neural models trained by the LM and BR algorithms are better than those of the neural models trained by QN, CGF, and SCG algorithms. The neural results have also been compared with the results of the respective quasi-static analysis and the synthesis formulas available in the literature. The proposed neural models for CPS synthesis are more accurate than the synthesis formulas available in the literature. The accuracy of the neural models trained by LM algorithm was found to be better than 0.24% for 10614 CPS samples having different electrical properties and geometrical dimensions. The neural models allow designers to obtain the physical dimensions of CPSs for the required design specifications in a very simple and convenient way, rather than using the iteration approach of applying conventional design equations. The method proposed here can easily be applied to other microwave problems. The high-speed real-time computation feature of the neural models recommends their use in MIC or monolithic MIC programs.

REFERENCES

1. Chiou, H. K., C. Y. Chang, and H. H. Lin, "Balun design for uniplanar broad band double balanced mixer," *Electronic Letters*, Vol. 31, 2113–2114, 1995.
2. Wen, C. P., "Coplanar waveguide: A surface transmission line suitable for nonreciprocal gyromagnetic device applications," *IEEE Transactions on Microwave Theory and Techniques*, Vol. 17, 1087–1090, 1969.
3. Ghione, G., "A CAD-oriented analytical model for the losses of general asymmetric coplanar lines in hybrid and monolithic MICs," *IEEE Transactions on Microwave Theory and Techniques*, Vol. 41, 1499–1510, 1993.
4. Chen, E. and S. Y. Chou, "Characteristic of coplanar transmission lines on multilayer substrates: Modelling and experiments," *IEEE Transactions on Microwave Theory and Techniques*, Vol. 45, 939–945, 1997.
5. Bedair, S. S., "Characteristic of some asymmetrical coupled transmission lines," *IEEE Transactions on Microwave Theory and Techniques*, Vol. 32, 108–110, 1984.
6. Ghione, G. and C. Naldi, "Analytical formulas for coplanar lines in hybrid and monolithic MICs," *Electronic Letters*, Vol. 20, 179–181, 1984.
7. Knorr, J. B. and K. D. Kuchler, "Analysis of coupled slots and coplanar strips on dielectric substrate," *IEEE Transactions on Microwave Theory and Techniques*, Vol. 23, 541–548, 1975.
8. Phatak, D. S. and A. P. Defonzo, "Dispersion characteristic of optically excited coplanar striplines," *IEEE Transactions on Microwave Theory and Techniques*, Vol. 38, 654–661, 1990.
9. Phatak, D. S., N. K. Das, and A. P. Defonzo, "Dispersion characteristic of optically excited coplanar striplines: Comprehensive full-wave analysis," *IEEE Transactions on Microwave Theory and Techniques*, Vol. 38, 1719–1730, 1990.
10. Deng, T. Q., M. S. Leong, P. S. Kooi, and T. S. Yeo, "Synthesis formulas for coplanar lines in hybrid and monolithic MICs," *Electronic Letters*, Vol. 32, 2253–2254, 1996.
11. Yildiz, C., "New and very simple synthesis formulas for coplanar strip line," *Microwave and Optical Technology Letters*, Vol. 44, 199–202, 2005.
12. Yildiz, C., A. Akdagli, and M. Turkmen, "Simple and accurate synthesis formulas obtained by using a differential evolution algorithm for coplanar strip lines," *Microwave and Optical*

Technology Letters, Vol. 48, 1133–1137, 2006.

13. Haykin, S., *Neural Networks: A Comprehensive Foundation*, Macmillan College Publishing Comp., New York, USA, 1994.
14. Watson, M. and K. C. Gupta, "Design and optimization of CPW circuits using EM-ANN models for CPW components," *IEEE Transactions on Microwave Theory and Techniques*, Vol. 45, 2515–2523, 1997.
15. Sagiroglu, S. and C. Yildiz, "A multilayered perceptron neural network for a micro-coplanar strip line," *Electromagnetics*, Vol. 22, 553–563, 2002.
16. Yildiz, C., S. Gultekin, K. Guney, and S. Sagiroglu, "Neural models for the resonant frequency of electrically thin and thick circular microstrip antennas and the characteristic parameters of asymmetric coplanar waveguides backed with a conductor," *AEÜ-International Journal of Electronics and Communications*, Vol. 56, 396–406, 2002.
17. Yildiz, C., S. Sagiroglu, and O. Saracoglu, "Neural models for coplanar waveguides with a finite dielectric thickness," *Int. J. RF and Microwave CAE*, Vol. 13, 438–446, 2003.
18. Yildiz, C., S. Sagiroglu, O. Saracoglu, and M. Turkmen, "Neural models for an asymmetric coplanar stripline with an infinitely wide strip," *International Journal of Electronics*, Vol. 90, 509–516, 2003.
19. Yildiz, C., S. Sagiroglu, and M. Turkmen, "Neural model for coplanar waveguide sandwiched between two dielectric substrates," *IEE Proc-Microwaves Antennas and Propagation*, Vol. 151, 7–12, 2004.
20. Devabhaktuni, K., M. C. E. Yagoub, Y. Fang, J. Xu, and Q. J. Zhang, "Neural networks for microwave modeling: Model development issues and nonlinear modeling techniques," *Int. J. RF and Microwave CAE*, Vol. 11, 4–21, 2001.
21. Watson, P. M., C. Choonsik, and K. C. Gupta, "Electromagnetic-artificial neural network model for synthesis of physical dimensions for multilayer asymmetric coupled transmission structures," *Int. J. RF and Microwave CAE*, Vol. 9, 175–186, 1999.
22. Salivahanan, S., R. Ramesh, S. Karthikeyan, S. Raju, and V. Abhaikumar, "CAD models for coplanar waveguide synthesis using artificial neural networks," *IETE Technical Review*, Vol. 18, 123–129, 2001.
23. Yildiz, C. and M. Turkmen, "Very accurate and simple CAD models based on neural networks for coplanar waveguide

synthesis," *Int. J. of RF and Microwave CAE*, Vol. 15, 218–224, 2005.

24. Salivahanan, S., R. Ramesh, S. Karthikeyan, S. Raju, and V. Abhaikumar, "Artificial neural network models for coplanar stripline synthesis," *IETE Journal of Education*, Vol. 43, 27–31, 2002.
25. Hagan, M. T. and M. Menjah, "Training feedforward networks with the Marquardt algorithm," *IEEE Transactions on Neural Networks*, Vol. 5, 989–993, 1994.
26. Mackay, D. J. C., "Bayesian interpolation," *Neural Computation*, Vol. 4, 415–447, 1992.
27. Gill, P. E., W. Murray, and M. H. Wright, *Practical Optimization*, Academic Press, New York, 1981.
28. Fletcher, R. and C. M. Reeves, "Function minimization by conjugate gradients," *Comput. J.*, Vol. 7, 149–154, 1964.
29. Moller, M. F., "A scaled conjugate gradient algorithm for fast supervised learning," *Neural Networks*, Vol. 6, 525–533, 1993.
30. Zhang, Q. J. and K. C. Gupta, *Neural Networks for RF and Microwave Design*, Artech House, 2000.
31. Christodoulou, C. G. and M. Georgiopoulos, *Application of Neural Networks in Electromagnetics*, Artech House, MA, 2001.
32. Guney, K., C. Yildiz, S. Kaya, and M. Turkmen, "Artificial neural networks for calculating the characteristic impedance of air-suspended trapezoidal and rectangular-shaped microshield lines," *Journal of Electromagnetic Wave and Applications*, Vol. 20, 1161–1174, 2006.
33. Jin, L. C., L. Ruan, and L. Y. Chun, "Design E-plane bandpass filter based on EM-ANN model," *Journal of Electromagnetic Wave and Applications*, Vol. 20, 1061–1069, 2006.
34. Mohamed, M. D. A., E. A. Soliman, and M. A. El-Gamal, "Optimization and characterization of electromagnetically coupled patch antennas using RBF neural networks," *Journal of Electromagnetic Wave and Applications*, Vol. 20, 1101–1114, 2006.
35. Thomas, V., et al., "A novel technique for localizing the scatterer in inverse profiling of two dimensional circularly symmetric dielectric scatterers using degree of symmetry and neural networks," *Journal of Electromagnetic Wave and Applications*, Vol. 19, 2113–2121, 2005.